

Transfer of shear stresses at steel-concrete interface

Peer-reviewed author version

Chrzanowski, M.; Odenbreit, C.; Obiala, R.; Bogdan, T. & DEGEE, Herve (2019)

Transfer of shear stresses at steel-concrete interface. In: Steel construction, 12(1), p. 44-54.

DOI: 10.1002/stco.201800024

Handle: <http://hdl.handle.net/1942/27991>

Maciej Chrzanowski*
 Christoph Odenbreit
 Renata Obiala
 Teodora Bogdan
 Hervé Degée

((Footnote))

* Corresponding author: maciej.chrzanowski@uni.lu

Transfer of the shear stresses at the steel-concrete interface.

Experimental tests and literature review.

Shear stresses can be transferred, via bond, at the steel-concrete interface without consideration of any mechanical shear connectors. The conducted research shows that the usage of anti-adhesive products, like grease, reduce the bond at the steel-concrete interface in push-out tests (POT). However, the effect is still significant, especially for fully encased steel profiles. The results of an experimental POT campaign with 9 small-scale cube specimens and 2 composite column specimens are presented. Three different surface conditions have been examined: (a) an untreated surface, (b) an anti-adhesive agent treated surface (formwork release oil) and (c) a PTFE-Spray treated surface. The resulting ultimate shear stresses were compared to the experimental results available in literature [1-10]. The influence of the different geometries of the specimens, the concrete age and the surface treatment conditions on the bond strength are compared and summarized.

1 Introduction

Tall buildings are rising higher and higher and the structural members of such buildings have to resist increasing forces. The technology allowing for such development evolves faster than the design standards and norms. The research presented hereafter focuses on composite columns. Heavy vertical members are the backbone of the tall buildings and their design goes far beyond the state of the current design codes. For example, in the current EN1994-1-1 [11], cross-sections with only one implemented steel profile and double symmetry are foreseen. While, in many buildings around the world, heavy composite column members with multiple separately encased steel profiles are used (see Fig. 1). Typically, the force transfer between the steel profile and the concrete, which ensures composite actions, is realized by mechanical shear connectors, mostly the shear studs.

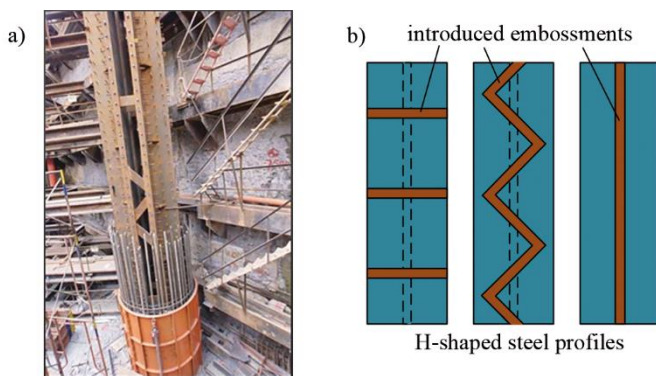


Fig. 1. Shear connection in composite columns – a) construction detail of the IFC Tower 2, Hong Kong (Source: Raymond Wong) and b) the investigated concept in terms of optimisation of the mechanical shear connection [12].

To transfer the shear forces between steel and concrete load-bearing elements of composite columns, different mechanical shear connectors are used. The load-bearing capacity of these connectors can be determined with laboratory tests, for example with the push-out test. The measured shear resistance of the connection consists of the mechanical part and bond on the surface between the materials. It has been concluded, that for the analytical evaluation of test results and understanding of the long term behaviour of the connection it is important to distinguish between the part of the load, which is transferred by the mechanical shear connector and the part, which is transferred by direct bond between concrete and steel surface.

The interest of this research was to identify resistance of the mechanical shear connector, which has been recently developed by Chrzanowski et al. [12], see Fig. 1b. Therefore, the layout of the structural test should be designed in a way that the shear force transfer by the bond is minimised by an appropriate surface treatment. In the common practice, the steel-concrete bond is neglected in the experimental testing of shear connectors by applying grease. However, based on this assumption, the load bearing capacity and initial stiffness of the mechanical shear connectors, especially for push-out type tests for in concrete embedded columns, could be overestimated. After greasing of the steel profile, the bond at the interface is reduced, but not

equal to zero and its contribution to the force transfer mechanism may still be significant [13]. Consequently, number of tests have been performed to evaluate the pure steel-concrete bond strength without any mechanical shear connection. An accurate evaluation of forces, transferred by the bond, allows getting a better insight into the mechanical connection mechanism and better assessment of its resistance [12-13].

As shown later, it is impossible to eliminate the bond fully, therefore, it is for the later test evaluation indispensable to know the part of the shear force, which was transferred by bond. Shear forces at the steel-concrete interface due to bond are transferred by two phenomena: (i) chemical adhesion and (ii) friction. Within the friction phenomenon itself, two major mechanisms have to be distinguished: (a) the Coulomb friction and (b) the surface roughness friction. Activation of the Coulomb friction requires always a normal force acting perpendicular on a surface, whereas the surface roughness friction can be obtained without any external pressure when two sliding surfaces are in contact. This effect has been investigated among others by Goralski [14].

2 Test campaign overview

9 small-scale cube push-out tests (SSCPOT) and 2 column type push-out tests (CoPOT) have been performed within a test campaign of the research project MultiCoSteel in the engineering structures laboratory of the University of Luxembourg, see Table 1. Both test series were reflecting the same type of specimens, where the steel part was fully embedded into the concrete block. The SSCPOT series were incorporating 3 different surface treatment conditions in order to analyse the shear stresses reduction due to the applied different bond reducing products. In addition, no concrete confinement has been introduced in the form of reinforcement bars. The series CoPOT investigated only a surface treated specimens with release agent oil, in which, a reinforcement cage has been included. At the bottom of each specimen, a recess has been placed in order to allow a free downward slide of the steel part, see Fig. 2 and Fig. 3. In both test series, the embedded steel parts have not been subjected to any cleaning processes and they have been applied to the specimens in the state 'as delivered', including the surfaces imperfections created during the milling process.

2.1 Geometry and material properties of the small-scale cube push-out tests – SSCPOT

The SSCPOT experimental test series contained 9 specimens with nominally identical geometry and material properties. The specimens only varied by the steel surface treatment conditions: untreated (PS), greased with oil (G) and Teflon coated (PTFE). The test specimens have been composed of two parts: a concrete cube with dimensions of 150x150x150 mm and an embedded steel bar with a rectangular cross-section of 10x30mm and a length of 150 mm. The embedded length of the steel bar was 100 mm. The applied steel bars have been cut from one bigger steel bar. The geometry of the specimen is shown in Fig. 2.

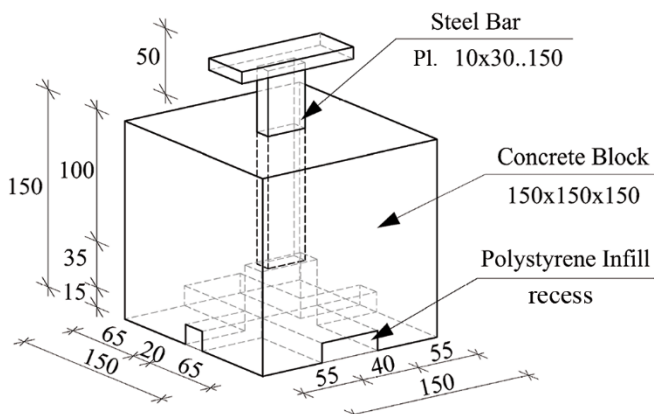


Fig. 2. Geometry of the SSCPOT specimen.

Material properties of the tested specimens were based on the normative values for steel S235JR according to EN 10025-1:2004 [15] and for concrete C35/45 according to EN 206-1:2000 [16] with the concrete manufacturer certificate, received upon delivery. The age of the concrete on the testing day was 21 days.

2.2 Geometry and material properties of the column push-out tests – CoPOT

In the CoPOT test series, 2 nominally identical test specimens have been fabricated and tested. The geometry of the specimens contained a centrally embedded steel profile HEB120, L=550 mm and a reinforced concrete block with dimensions of 340x1000x450 mm. The embedded length of the steel profile was 350 mm. In both cases, the steel surface treatment process was identical – no cleaning process has been applied beforehand and the steel profile has been coated with an anti-adhesive release oil, like in the G series of SSCPOT. The geometry of the specimens is shown in Fig. 3.

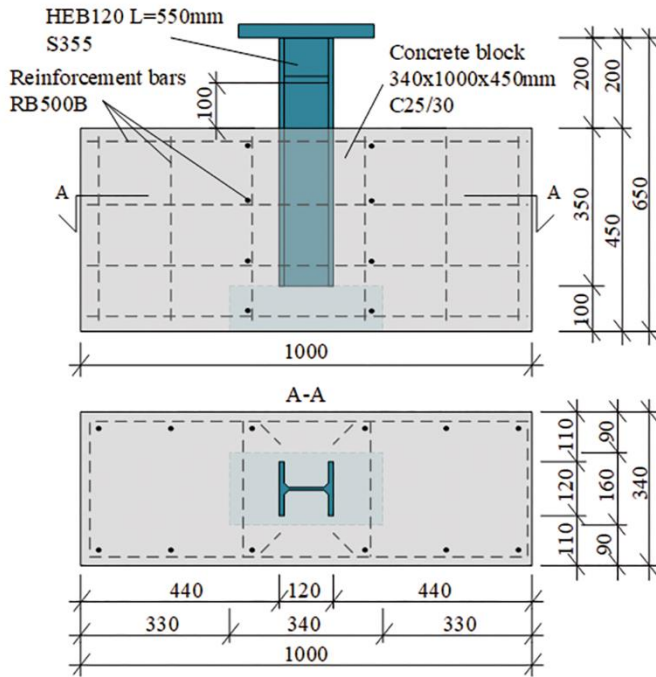


Fig. 3. Geometry of the CoPOT specimen.

The reinforcement of each specimen were identical and contained three types of bars: (1) longitudinal bars 12 Ø10, L=380 mm, (2) transversal stirrups 4 Ø12, L=2615 mm and (3) U-hoop bars around the steel profile 8 Ø12, L=525 mm, see Fig. 3.

All characteristic material properties for structural steel, reinforcement steel and concrete have been experimentally obtained according to normative testing procedures described in ISO 6892-1:2009 [17], ISO 6935-2:2007 [18] and EN 12390-3:2001 [19], respectively. The structural steel grade was S355JR+M and the measured properties were 455 MPa for yielding strength, 527 MPa for tensile strength, 208 GPa for elastic modulus and 26.5% elongation at fracture. The reinforcement steel grade was RB500B and the measured properties were 565 MPa for yielding strength, 665 MPa for tensile strength, 206 GPa for elastic modulus and 29% elongation at fracture. The manufacturer certificate received upon delivery supports the concrete properties and the measured mean compression strength after 28 days were 41 MPa for the cylinders and 45 MPa for the cubes.

3 SSCPOT – fabrication, test conduction and results

Securing the precise vertical orientation of the embedded steel bar, as shown in Fig. 2, was a key point during the fabrication process. Due to special fixation, the steel bars have been prevented from any movement during concreting. No cleaning process of the steel parts has been applied beforehand.

In the PS series (see Table 1), no bond-reducing coating has been applied and represents the reference tests. The bond reducing product applied in the G-series was a high-performance anti-adhesive release agent “WETCAST – FormFluid HP” of the Hebau company and of the PTFE-series was a PTFE-spray of the KimTec company, which builds a solid coating after curing. The steel bars of the G series were painted profusely approximately 4 hours before the concreting with the oil, using a paintbrush, whereas the PTFE coating has been applied uniformly with a sprayer (1-2 layers – approx. 25-40 µm) the day before concreting.

The Zwick Roell Testing Machine of 400 kN nominal capacity has been used to perform the push-out tests (Type 065146.100, Series No. 807289/02). The test layout is shown in Fig. 4. The load was applied in form of a ramp in the displacement control mode to the top of the steel bar. The loading rate in the first phase has been defined as 0.2 mm/min (machine travel) until the force level of 20kN has been reached. After this point, the travel rate was increased to 0.5 mm/min. The tests have been stopped when the force dropped more than 10% below the peak load.

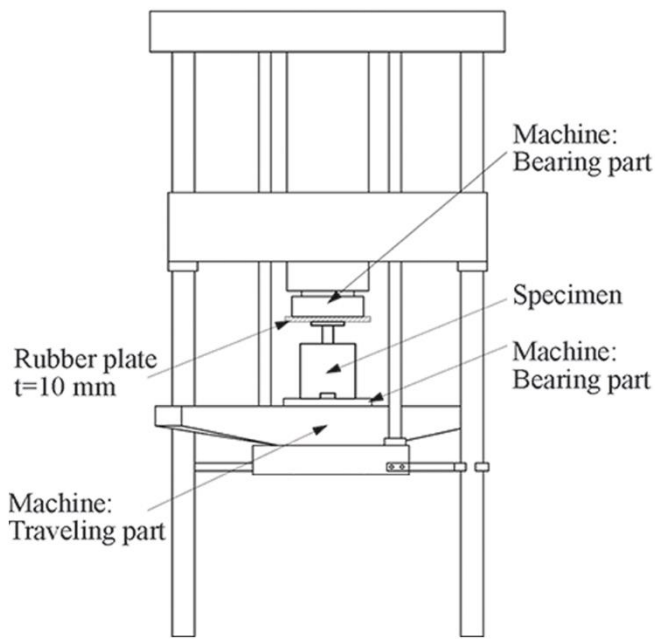


Fig. 4. SSCPOT test setup scheme.

The small scale of the SSCPOT specimens do not allowed for placing a linear variable transducers to measure the relative slip between the steel bar and concrete block. In result, during the test conduction, the displacement and corresponding load of the machine have been recorded. Due to a large stiffness of the testing machine and the small loads, the displacement of the machine was set equal to the relative slip between steel and concrete parts of the tested specimens. An error of the recorded data on the measured relative slip and corresponding load has been neglected by correction displacements in function of the imposed load obtained from the compliance test of the machine.

All test series showed similarities but also significant differences in the load-slip behaviour. In the initial phase, a nearly linear elastic behaviour has been observed with a sudden load drop at different point for all specimens, where for the series G, the load drop was barely visible and it occurred at the relative slip level of approximately 0.5 mm, as shown in Fig. 5. This drop is explained by a steel-concrete adhesive chemical debonding. In the second phase, considered after the drop, for the PS and G series the load-bearing resistance is increasing again, even above the first peak load due to the friction between the steel and concrete materials. On the contrary for the PTFE series, the load increase after debonding did not occur. The third phase is considered after reaching the maximum load, where the load is reducing with increasing slip similarly for all the tests. The slopes of the descending branches showed a certain level of ductility, which proved the existence of the surface-roughness friction. The experimentally obtained load slip responses are presented in Fig. 5. A summary of the results is given in Table 2.

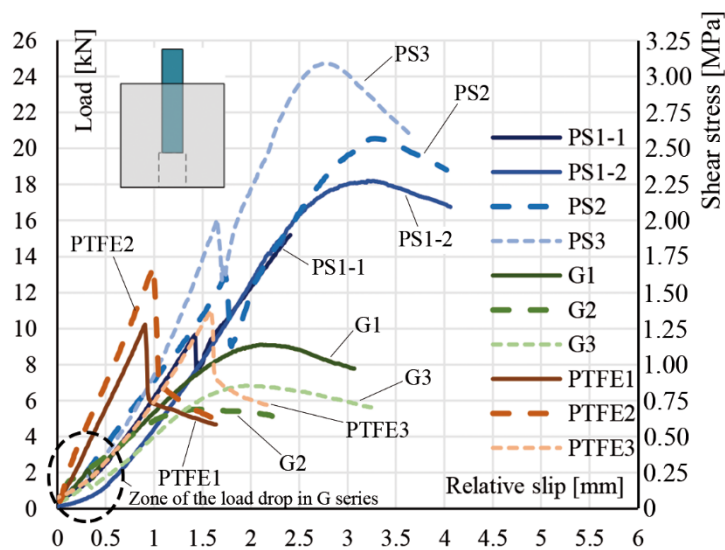
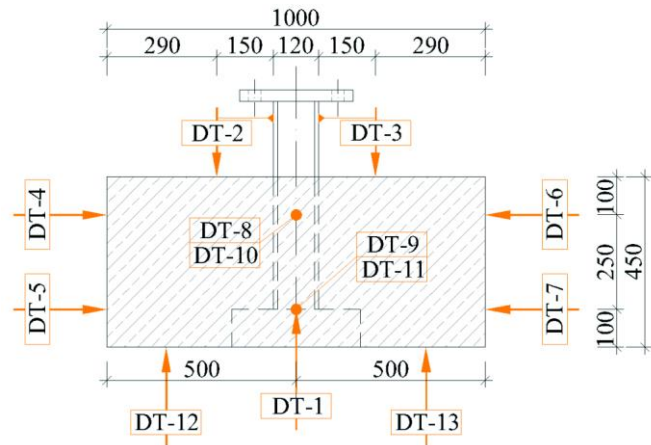


Fig. 5. Experimental SSCPOT load-slip curves.

4 CoPOT – fabrication, test conduction and results

The two column type push-out test specimens CoPOT, as described in Table 1 on the row 0v2, have been assembled from three main parts: (i) the HEB120 steel profiles, (ii) the reinforcement cages and (iii) the C25/30 concrete blocks. No surface cleaning process has been applied to the steel profiles. A coating with the same anti-adhesive release agent WETCAST FormFluid HP as for test specimens SSCPOT, series G, has been applied to both specimens. A special care was taken during the fabrication process to ensure verticality of the steel profile.

All CoPOT tests were instrumented with a set of 13 displacement transducers (DT) and a set of 2 strain gauges (SG) glued to steel profiles as shown in Fig. 6 and Table 3. To measure the relative slip between the steel profile and the concrete block, two DTs have been fixed with the plastic clamps to the supporting bars welded to the steel profile. The aforementioned DTs have been pointed to the top surface of the concrete, see Fig. 6, DT-2 and DT-3. The reference point of the displacement transducers DT-1, DT-12 and DT-13 was the ground and they were used to measure relative displacement between the bottom part of the steel profile and the concrete block to eliminate eventual deformation of the supporting frame.



(Table 3. here on the side)

Fig. 6. Scheme of the implemented displacement transducers in CoPOT, south face view.

The CoPOTs were executed with the usage of a hydraulic press of 1 MN nominal capacity. In both cases, test layout and setup were identical, see Fig. 7.

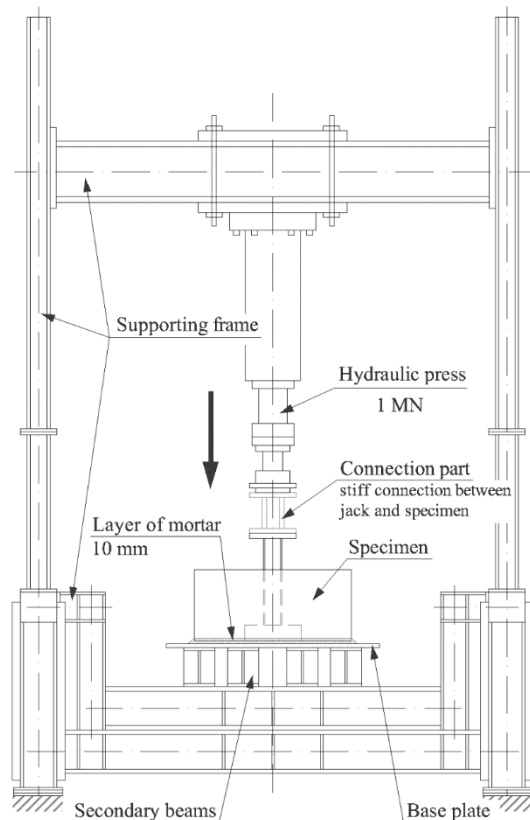
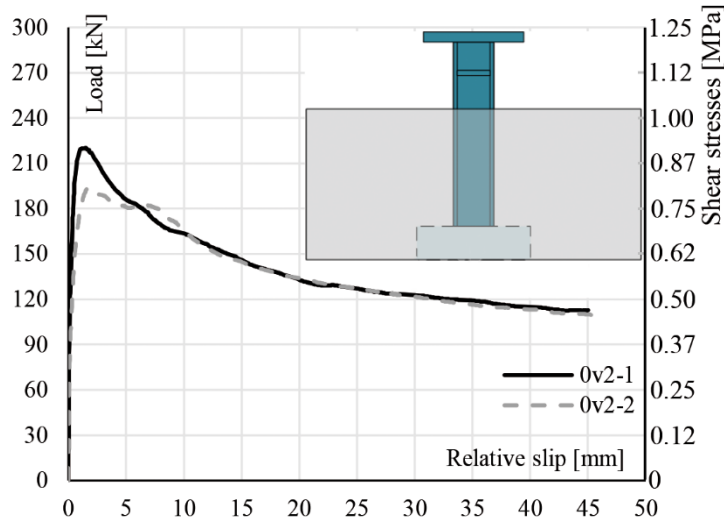


Fig. 7. CoPOT test setup scheme.

The test procedure of EN1994-1-1:2004, Annex B [11] has been applied. The tests have been conducted as displacement-controlled and the increments were in progressive steps. The displacement-rate was set at speed 0.5 mm/min at the hydraulic press. Between each load increment (approx. 30 kN), a pause of 4-5 min has been imposed in order to allow for a concrete relaxation and investigation of the load drop characteristic. After reaching 45% of the expected ultimate load, the specimens were subjected to 25 cycles between 5% and 40% of the expected ultimate load with the frequency of 0.015 Hz in the force control mode. After these load-cycles, the quasi-static increments were continued up to the failure of the specimens. After the maximum load was reached, the specimens were continuously loaded with a constant displacement up to approximately 45mm relative slip.

The recorded data has been post-processed and the load-slip diagram is shown in Fig. 8. The shown slip is evaluated as the average signal of the sensors DT-2 and DT-3, see Fig. 6. The characteristic values are summarized in Table 4.



(Table 4. here on the side)

Fig. 8. CoPOT experimental load-slip curves.

The examination of the tested specimens showed no visual concrete damage. After reaching the ultimate load, the adhesive part of the force transfer started to decrease and only the inelastic surface roughness friction between two parts remained active.

Based on the analysis of the measurement recorded by the strain gauges (SG) during the CoPOT tests, a nearly linear distribution of the stresses along the height of the embedded steel profiles can be assumed, see Fig. 9b. In turn, it can lead to the simplified assumption that the shear stresses at the steel-concrete interface are uniformly distributed over the whole contact area. The results, at the stage before the failure of the specimen, have been compared with other tests found in literature and similar conclusions have been presented by Roeder et al. [3].

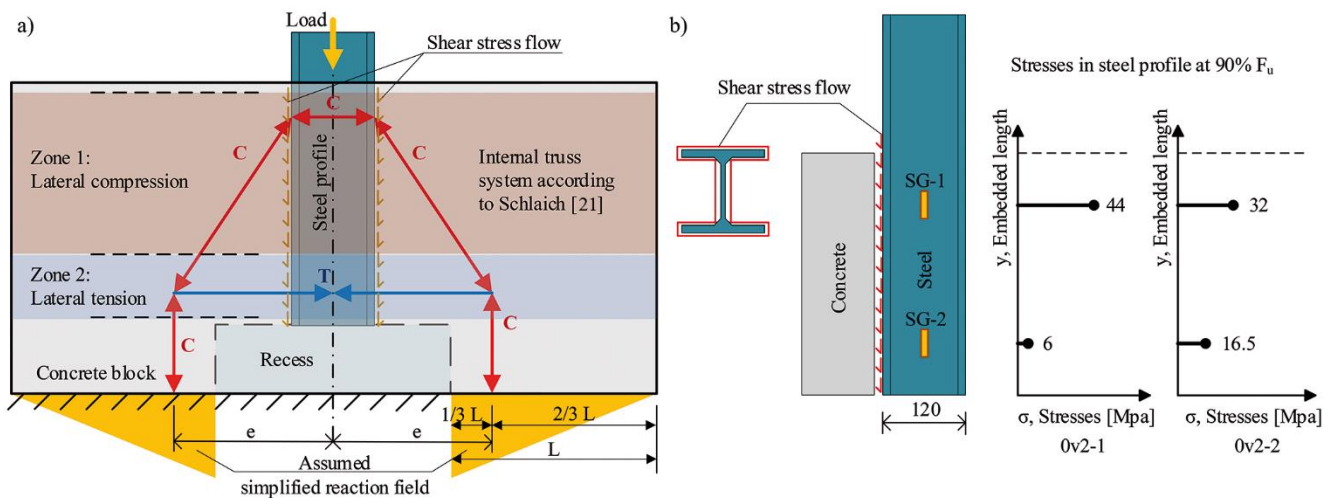


Fig. 9. CoPOT force transfer mechanism – a) simplified strut and tie model and b) measured stresses within the steel profile.

The evaluation of the test results showed, that all three mechanisms of the steel-concrete bond have been activated. In the initial test phase, the forces at the interface were transferred by the chemical adhesion phenomenon. This branch of the load-slip curve is characterised by a high stiffness and a nearly linear behaviour. This corresponds well to the theoretical model according to the traction-separation law of the fracture mechanics, as described

for example in the Fib Bulletin 72 [20]. Near the ultimate load, a smoothed character of the load-slip curves was observed, which indicates certain ductility and it is in clear contradiction to the brittle behaviour of an adhesive failure. This effect can be explained by an activation of the Coulomb friction mechanism.

According to Schlaich [21], the eccentricity “e” of the support conditions, as indicated in Figure 9a, allows for a development of transversal compression in the system, which creates two general zones, compression and tension zones, to balance the internal forces. In the result, with increasing loading force, the compression in the Zone 1 increases a pressure on the surface between the concrete and steel and proportionally increases the Coulomb friction force. At the maximum load, the shear force is composed of adhesion and Coulomb friction forces. Based on the above stated, it could be concluded that the imposed boundary conditions and size of the eccentricity of the support conditions have a direct impact on the ultimate bond shear resistance. Analysis of the load-slip response given in Fig. 8 shows that the bond damage and the shear connection failure does not occurs in a brittle manner, but it is smoothed over the progressing relative slip. This can be explained by the fact that the adhesion failure is not occurring at the same time over the total embedded length of the steel profile. The adhesive bond failure will start in the lower part of the steel profile where the lateral tension has been developed, Zone 2 in Fig. 9a, and further progress upward. In the result, with diminishing adhesion part of the bond along the steel-concrete interface, the Coulomb friction force is dropping due to the reduced transversal compression level in Zone 1. After the peak load is reached, the adhesion part of bond is vanished and the shear transfer at the interface is composed only of the remaining Coulomb friction part and surface roughness friction part. The descending branch of the load-slip curve beyond a displacement of 5mm indicates, that even the surface roughness friction part of the shear resistance is not a constant, but depending on and decreasing with the increasing displacement towards a constant value.

5 Test results evaluation

As mentioned above, the steel-concrete bond is defined as the tangential shear resistance due to the chemical adhesion and friction phenomena at the steel-concrete interface. A relation between the force acting on a specified contact area and the resulting shear stresses can be defined in Eq. 1 with a simplified assumption, based on the observations given in Fig. 9b, of an equal shear stress distribution over the whole contact area of the profile. The effective steel-concrete contact area is defined in Eq. 2.

$$\tau_{surf,i} = \frac{F_i}{A_{c,eff}} \left[\text{kN/cm}^2 \right] \quad (1)$$

$$A_{c,eff} = L_{emb,s} \cdot u_{s,eff} \left[\text{cm}^2 \right] \quad (2)$$

Where,

$L_{emb,s}$ is the embedded length of the steel part, for the SSCPOT it was 100mm and for the CoPOT 350 mm;

$u_{s,eff}$ is the effective embedded perimeter of the steel part, for the SSCPOT it was 80 mm and for the CoPOT 686 mm.

The effective contact area for SSCPOT test series is 80 cm² and 2401 cm² for CoPOT test series. The effective areas and the ultimate loads of the experimental tests allow to calculate the steel-concrete bond strength values according to Eq. 1. The obtained results are summarized in Table 5.

6 Comparison of the results with literature data

Additional data of bond strength between steel and concrete and influence of different parameters has been found in literature. The data is summarised in Table 6.

Based on the conducted tests and the literature review [1-10], it can be stated that the steel-concrete bond is sensitive to various parameters such as steel surface treatment, concrete cover thickness, level of the concrete confinement, geometry of the specimens, boundary conditions or the time. Therefore, the bond strength values cannot be directly extrapolated to specimens with different geometry and conditions. In addition, the contribution of the steel-concrete bond in the force transfer mechanism of shear connectors in push-out tests with embedded steel profiles is significant (even for greased surfaces) and it cannot be disregarded. The influence of the most important parameters is discussed below:

Influence of the steel surface treatment

The most critical influence on the steel-concrete bond strength has the steel surface treatment. It could be observed that the specimens with rusted steel surface reached the highest bond strength, see Table 6, No.7. Furthermore, specimens with surface failure scales from rolling process indicated higher resistance than specimens with cleaned steel surface (sandblasted or paint thinner), see Table 5, No.1 and Table 6, No.3. The poorest resistance properties were noticed in specimens with “greased” steel surface, but the values were still significant, see Table 5, No.2. Paint or Teflon coatings (similar

bond strength reducing properties) were not as efficient in reducing the bond strength as the greasing process, see Table 5, No.3 and Table 6, No.7.

Influence of the concrete cover

Second, the most impacting parameter on the bond strength was concrete cover thickness. A thin concrete cover (around 50 mm) and a big steel-to-concrete surface ratio in composite cross-section resulted in weak shear resistance of bond, see Table 6, No.3 or 4. At the same time, specimens with a thick concrete cover (over 100 mm) and a small steel-to-concrete surface ratio in composite cross-section reached high bond stress values, see Table 6, No.6. Concrete shrinkage could have a positive or negative influence on the steel-concrete bond strength, depending on the geometry of the specimen (embedded or filled steel profiles with concrete) or if shrinkage creates tension or compression orthogonal to the contact surface, see Table 6, No.1.

Influence of the concrete confinement

Concrete confinement affects the frictional behaviour of the steel-concrete bond. The higher confinement of the concrete, the higher shear resistance at the steel-concrete interface can be observed, see Table 6, No.5. A big impact on the resulting bond strength values could be observed when a lateral pressure to the interface occurred – for example transversal reinforcement anchoring tensile forces from compression struts, like for example in push-out tests of shear connectors. The existence of a transversal reinforcement without imposing a lateral pressure has a minor effect on the steel-concrete bond.

Influence of the geometry of the steel profile

The geometry of the steel profile has an impact on the concrete confinement level and confinement zones, for example zones between flanges of the H-shaped steel profiles or concrete-filled tube specimens. Thus, an impact on the bond strength values are noticeable. It was observed that the steel-concrete bond strength (stress values) is reduced with increased scale of the implemented steel profiles, see Table 5 and Table 6, No.4.

Influence of the time

In tests performed by Wium [2], it could be observed that the steel-concrete bond has been affected by the age of the specimen. The difference between two nominally identical specimens, tested with the time space of 6 months, resulted in the reduced values of bond by approximately 15%. This effect should be associated with creep and shrinkage effects, but it is not investigated further in this article.

7 Summary and conclusions

The presented article describes the steel-concrete bond phenomenon between the plain steel and concrete surfaces in steel-concrete composite structures. The focus of the investigation is put on fully embedded steel profiles like for example in composite columns. The impact on the bond behaviour due to the different conditions is explained. The steel-concrete bond shear strength has been evaluated from the experimental tests performed within the presented research project and compared with international literature. A good correlation between SSCPOT G series and CoPOT series could be observed. It has been shown, that the anti-adhesive release agent has a better bond reducing property than the Teflon coating (stresses reduction for WETCAST-FormFluid HP product reached 66% - in comparison to PS series). In series G and PTFE, the level of the residual strength was similar. From the executed experimental tests, the ultimate bond strength values are: (i) for PS series – 2.65 MPa, (ii) for G series – 0.9 MPa, (iii) for PTFE series – 1.47 MPa, and (iv) for 0v2 series – 0.86 MPa.

Moreover, it has been confirmed by results found in literature that the steel-concrete bond strength is not a universal value and it is sensitive to different parameter. The highest values of the bond strength were noticed for the specimens with rusted steel surface – 2.91 MPa, SmartCoCo [5], and/or a big concrete cover (around 100mm or more) – 5.51 MPa, Xing et al. [4]. The smallest resulting stresses have been obtained for the specimens with thin concrete cover (around 50mm) – 0.45 MPa, Roik [1], and with applied bond-reducing products on the cleaned steel surface – 0.12 MPa, Roik [1].

An arrangement of the transversal reinforcement has a minor effect on the steel-concrete bond strength but can significantly affect the concrete confinement level and impose a lateral pressure and amplify the friction effect. Wium [2] showed that the bond strength is reducing within the time.

In summary, it was observed that the bond strength is strongly sensitive to the size of the concrete encasement, the steel surface treatment conditions, the concrete confinement level, existence of the lateral forces, the geometry of the specimen and age of the concrete. Therefore, the acquired bond strength results cannot be extrapolated directly to specimens in different scale and condition. Moreover, excluding the aspect of geometry of specimens, the steel-concrete bond cannot be completely eliminated by a greasing of the steel profiles, especially not for the fully embedded steel profiles, due to irregularities on the surface of the steel profiles and remaining chemical adhesive strength.

Acknowledgements

The presented research project MultiCoSteel, is running in close collaboration with the industrial project partner ArcelorMittal Global R&D – Construction & Infrastructure Applications Department, Luxembourg. It is funded and supported by the Luxembourgish National Research Fund within the scheme of the FNR AFR-PPP PhD Grant (Call 2016-1), Project Reference 11283614. Numerical experiments presented in this paper were carried out using the HPC facilities of the University of Luxembourg, see <http://hpc.uni.lu>.

References

- [1] Roik K.: *Untersuchung der Verbundwirkung zwischen Stahlprofil und Beton bei Stützenkonstruktionen*. Studiengesellschaft für Anwendungstechnik von Eisen und Stahl e.V., Düsseldorf, 1984.
- [2] Wium J.A.: *Composite Columns: Force Transfer from Steel Section to Concrete Encasement*. Thèse No 1008 (1992), Ecole Polytechnique Fédérale de Lausanne, 1992..
- [3] Roeder C.W.; Chmielowski R.; Brown C.B.: Shear Connector Requirements for Embedded Steel Sections. *Journal of Structural Engineering*, 125(2):142-151, 1999.
- [4] Xing G.; Zhou C.; Wu T.; Liu B.: Experimental Study on Bond Behaviour between Plain Reinforcing Bars and Concrete. *Advances in Materials Science and Engineering*, Vol. 2015, <http://dx.doi.org/10.1155/2015/604280>.
- [5] Degée H.; Plumier A.; Bogdan T.; Popa N.; Cajot L.-G.; De Bel J.-M.; Menegeot P.; Hjjaj M.; Nguyen Q.-H.; Somja H.; Elghazouli A.; Bompa D.: *Smart Composite Components – Concrete Structures Reinforced by Steel Profiles, SmartCoCo*. European Commission, Research Programme of the Research Funds for Coal and Steel, TGS 8, Grant Agreement RFSR-CT-2012-00031, 2016.
- [6] Tao Z.; Song T.Y.; Uy B.; Han L.H.: Bond behaviour in concrete-filled steel tubes. *Journal of Constructional Steel Research*, 120, 81-93, 2016.
- [7] Pecce M.; Ceroni F.: Bond tests of partially encased composite columns. *Advanced Steel Construction Journal*, Vol. 6, No. 4, 1001-1018, 2010.
- [8] Xu K.-C.; Chen M.-C.; Yuan F.: Confined Expansion and Bond Property of Micro-Expansive Concrete Filled Steel Tube Columns. *The Open Civil Engineering Journal*, 5, 173-178, 2011.
- [9] De Nardin S.; El Debs A.L.H.C.: Shear transfer mechanisms in composite columns: an experimental study. *Steel and Composite Structures Journal*, Vol. 7, No. 5, 377-390, 2007.
- [10] Mollazadeh M.H.: *Load Introduction into Concrete-Filled Steel Tubular Columns*. PhD Thesis, University of Manchester, UK, 2015.
- [11] EN 1994-1-1. Eurocode 4: Design of composite steel and concrete structures – Part 1-1: General rules and rules for buildings. European Standard, European Committee for Standardization, Brussels, Belgium, 12.2004.
- [12] Chrzanowski M.; Odenbreit C.; Obiala R.; Bogdan T.; Braun M.; Degée H.: Development of an innovative type of shear connector dedicated to fully embedded steel-concrete composite columns – experimental and numerical investigations. *Proceedings of the 12th International Conference on Advances in Steel-Concrete Composite Structures (ASCCS 2018)*, Valencia, Spain, 427-434, 2018.
- [13] Chrzanowski M.; Odenbreit C.; Obiala R.; Bogdan T.: Shear stresses analysis at the steel-concrete interface with the usage of bond eliminating products. *Proceedings of the XI Congresso de Construção Metálica e Mista (XICMM)*, Coimbra, Portugal, 1027-1036, 2017.
- [14] Goralski C.: *Zusammenwirken von Beton und Stahlprofil bei kammerbetonierten Verbundträgern*. Doktors Dissertation, Rheinisch-Westfälischen Technischen Hochschule Aachen, 2006.
- [15] EN 10025-1:2004. Hot rolled products of structural steels – Part 1: General technical delivery conditions. European Standard, European Committee for Standardization, Brussels, Belgium, 11.2004.
- [16] EN 206-1:2000: Concrete – Part 1: Specification, performance, production and conformity. European Standard, European Committee for Standardization, Brussels, Belgium, 12.2000.
- [17] ISO 6892-1:2009. Metallic materials – Tensile testing – Part 1: Method of test at room temperature. International Standard, International Organization for Standardization, Geneva, Switzerland, 08.2009.
- [18] ISO 6935-2:2007. Steel for the reinforcement of concrete – Part 2: Ribbed bars. International Standard, International Organization for Standardization, Geneva, Switzerland, 01.2007.

- [19] EN 12390-3:2001. Testing hardened concrete – Part 3: Compressive strength of test specimens. European Standard, European Committee for Standardization, Brussels, Belgium, 12.2001.
- [20] fib Model Code for Concrete Structures 2010. International Federation for Structural Concrete (fib), 2013.
- [21] Schlaich J.; Schäfer K.: Design and detailing of structural concrete using strut-and-tie models. *The Structural Engineer Journal*, Vol. 69, No. 6, 113-125, 03.1991.
- [22] Chrzanowski M.: *Shear transfer in heavy steel-concrete composite columns with multiple encased steel profiles (working title)*. PhD Thesis (in preparation), University of Luxembourg, Luxembourg, foreseen 07.2019.
- [23] EN 10088-4:2009. Stainless steels – Part 4: Technical delivery conditions for sheet/plate and strip of corrosion resisting steel for construction purposes. European Standard, European Committee for Standardization, Brussels, Belgium, 04.2009.

Keywords: steel-concrete composite columns; composite action; longitudinal shear; steel-concrete bond; shear stresses between plain steel and concrete surfaces; assessment of the steel-concrete bond strength; analysis of the steel-concrete bond behaviour;

Authors

M.Sc. Eng., Eng. Arch. Maciej Chrzanowski &
Prof. Dr.-Ing. Christoph Odenbreit
University of Luxembourg
RUES, FSTC, ArcelorMittal Chair of Steel and Façade Engineering
6, rue Richard Coudenhove-Kalergi
L-1359 Luxembourg-City, Luxembourg
maciej.chrzanowski@uni.lu
christoph.odenbreit@uni.lu

Renata Obiala, PhD
Teodora Bogdan, PhD
ArcelorMittal Global R&D
Construction & Infrastructure Applications Department
66, rue de Luxembourg
L-4009 Esch-sur-Alzette, Luxembourg
renata.obiala@arcelormittal.com
teodora.bogdan@arcelormittal.com

Prof. Dr. Ir. Hervé Degée
Hasselt University
FET, CERG
Martelarenlaan 42
3500 Hasselt, Belgium
herve.degee@uhasselt.be

List of Figures

Fig. 1. Shear connection in composite columns – a) construction detail of the IFC Tower 2, Hong Kong (Source: Raymond Wong) and b) the investigated concept in terms of **optimisation of the mechanical shear connection [12]**.

Fig. 2. Geometry of the SSCPOT specimen.

Fig. 3. Geometry of the CoPOT specimen.

Fig. 4. SSCPOT test setup scheme.

Fig. 5. Experimental SSCPOT load-slip curves.

Fig. 6. Scheme of the implemented **displacement transducers** in CoPOT, south face view.

Fig. 7. CoPOT test setup scheme.

Fig. 8. CoPOT experimental load-slip curves.

Fig. 9. CoPOT force transfer mechanism – a) simplified strut and tie model and b) measured **stresses** within the steel profile.

List of Tables

Table 1. Overview of test specimens.

Test Name	Geometry	Sub-number	Concrete Part	Steel Part	Embedded length / Contact area	Surf. Treatment	No of tests	Results
Test Series: SSCPOT (small scale cube push-out tests)								
PS	Fig. 2	-1	Cube:	Steel Bar:	100 mm	Cleaning: No	3	Fig. 5
		-2	150x150x150 mm	10x30x150 mm	/ 80 cm ²	Coating: No		
		-3	with 20x40x50 mm recession at the bottom					
G	Fig. 2	-1	Cube:	Steel Bar:	100 mm	Cleaning: No	3	Fig. 5
		-2	150x150x150 mm	10x30x150 mm	/ 80 cm ²	Coating:		
		-3	with 20x40x50 mm recession at the bottom			Release agent - oil		
PTFE	Fig. 2	-1	Cube:	Steel Bar:	100 mm	Cleaning: No	3	Fig. 5
		-2	150x150x150 mm	10x30x150 mm	/ 80 cm ²	Coating:		
		-3	with 20x40x50 mm recession at the bottom			PTFE Teflon Spray		
Test Series: CoPOT (large scale column type push-out tests)								
0v2	Fig. 3	-1	Reinforced concrete block:	Steel Profile:	350 mm	Cleaning: No	2	Fig. 8
		-2	340x1000x450 mm with 160x340x100 mm recession at the bottom	HEB120 L=550 mm	/ 2401 cm ²	Coating: Release agent - oil		

Table 2. SSCPOT test results summary.

Values	Unit	Untreated surface				Anti-adhesive oil treated surface				Teflon spray treated surface			
		PS1	PS2	PS3	Mean	G1	G2	G3	Mean	PTFE1	PTFE2	PTFE3	Mean
F_u	[kN]	18.32	20.58	24.74	21.21	9.12	5.53	6.89	7.18	10.39	13.65	11.18	11.74
F_{adh}	[kN]	9.79	13.10	16.22	13.04	2.24	1.51	1.48	1.74	10.39	13.65	11.18	11.74
δ_u	[mm]	3.20	3.27	2.79	3.09	2.15	1.47	2.19	1.94	0.92	1.00	1.60	1.18
δ_{adh}	[mm]	1.43	1.75	1.66	1.61	0.33	0.12	0.32	0.26	0.92	1.00	1.60	1.18
δ_1	[mm]	2.53	2.79	2.36	2.56	1.64	1.03	1.53	1.40	0.83	0.91	1.48	1.07
δ_2	[mm]	4.22	4.14	3.35	3.90	2.80	2.64	2.79	2.74	0.93	1.02	1.62	1.19
$\frac{\delta_2 - \delta_u}{\delta_u - \delta_1}$	[-]	1.52	1.80	1.29	1.53	1.27	2.64	0.92	1.61	0.13	0.17	0.14	0.15
K_{adh}	[kN/mm]	6.85	7.44	9.76	8.02	6.86	13.42	4.64	8.31	11.31	13.59	6.97	10.62
K_1	[kN/mm]	6.19	7.16	7.42	6.92	5.34	4.89	3.99	4.74	11.31	13.59	5.96	10.29

 F_u – Ultimate load F_{adh} – Load level at the adhesion mechanism failure δ_u – relative slip corresponding to the ultimate load level δ_{adh} – relative slip corresponding to the adhesion failure load level δ_1 – relative slip at $0.9F_u$, before failure δ_2 – relative slip at $0.9F_u$, after failure K_{adh} – Stiffness measured at δ_{adh} K_1 – Stiffness measured at the relative slip level of 1mm (for PTFE1 specimen measured at δ_u)

Table 3. Measurement equipment of CoPOT – Strain Gauges.

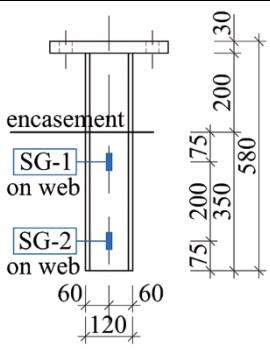
Strain Gauges placement scheme	No.	Sensor Name	Position
 <p>The diagram illustrates the placement of two strain gauges, SG-1 and SG-2, on the web of a steel profile. The profile has a total height of 580 mm and a total width of 120 mm. SG-1 is located 75 mm from the top flange and 200 mm from the bottom flange. SG-2 is located 75 mm from the bottom flange. The web thickness is 6 mm. The diagram also shows the 'encasement' area around the profile.</p>	1.	SG-1	Web of the steel profile - top
	2.	SG-2	Web of the steel profile - bottom

Table 4. CoPOT experimental test results.

Values	Unit	Specimen 0v2 series		Mean
		0v2-1	0v2-2	
F_u , Ultimate load (peak load)	[kN]	221	194	208
F_6 , Load level at 6 mm of relative slip	[kN]	182	182	182
δ_u , Relative slip at ultimate load	[mm]	1.49	1.64	1.56
δ_1 , Relative slip at $0.9F_u$, before failure	[mm]	0.52	0.93	0.72
δ_2 , Relative slip at $0.9F_u$, after failure	[mm]	3.43	6.95	5.19
$\frac{\delta_2 - \delta_u}{\delta_u - \delta_1}$	[-]	2.00	7.48	4.74
K_1 , Bond stiffness at $\delta = 1$ mm	[kN/mm]	216	178	197

Table 5. Steel-concrete bond strength comparison.

No.	Specimen and steel profile	Concrete	Surface treatment	Confinement	Embd. length	Effective area	Bond strength
SSCPOT							
1.	3x PS Steel bar 10x30x150	C35/45 Cube 150x150x150 Age: 21 days	No	Concrete cover: $c_x=70\text{mm}$, $c_y=60\text{mm}$	100 mm	80 cm ²	2.65 MPa
2.	3x G Steel bar 10x30x150		Anti-adhesive release agent (oil)				0.90 MPa
3.	3x PTFE Steel bar 10x30x150		Teflon spray cover approx. 25-40µm				1.47 MPa
CoPOT							
4.	2x 0v2 HEB 120 L=550 mm	340x1000x450 f_{cm} =41MPa Age: 28 days	Anti-adhesive release agent (demoulding oil agent)	Concrete cover: $c_x=440\text{mm}$, $c_y=110\text{mm}$ Stirrups: Ø12/117	350 mm	2401 cm ²	0.87 MPa

For a more detailed list and analysis of the steel-concrete bond, a reference to the Ph.D. Thesis of the author [22] is given.

Table 6. Steel-concrete bond – literature data.

No.	Specimen and steel profile	Concrete	Surface treatment	Confinement	Embd. length	Effective area	Bond strength
Roik [1]							
1.	84x Specimens on rectangular and circular steel tubes Rectangular D120-140 Circular Ø120-140	Tube infill $f_c = 53.4-72.4 \text{ MPa}$ Age: 34-598 days	Cleaned surface with paint thinner. Some tests without information + damaged interface by shrinkage.	External tube cover. rectangular circular	Between 120-280 mm	Between 529-1170 cm ²	Between *0.82-1.66 MPa (one series with 0.12 MPa)
2.	9x Specimens on HEB200 embedded steel profiles L=500 mm	B25/35 Block 330x330x470 Age: 31 days	Cleaned surface with paint thinner. Some tests coated with rust preventive paint, thickness 25-60 µm.	Concrete cover. 65 mm thick. Bugelmatte Q131: Ø5/150	440 mm	5060 cm ²	Between 0.7-1.40 MPa
3.	16x Specimens on embedded steel plate 16x300x300	B25/35 Block thick 75-256 mm 400x400 mm Age: 99 days	Mechanically cleaned. Cleaned surface with paint thinner. No coating.	Concrete cover. Dir. 1: 50 mm Dir. 2: 30-120 mm Stirrups: Ø6-8/37-150	300 mm	1896 cm ²	Between 0.45-1.06 MPa
Wium [2]							
4.	29x Specimens on embedded steel profiles HEB200 L=500 mm ~HEB200 L=1120 mm ~HEB400 L=1270 mm	Block between 330x330x470 to ~600x500x1150 $f_c = 36.5-44.1 \text{ MPa}$ Age: 28-169 days	Sandblasted Sa2.5 (Some specimens closed at the base by end-plate – no free relative slip possible)	Concrete cover. Dir. 1: 50-100 mm Dir. 2: 50-100 mm Stirrups: Ø8/100 (one series Ø8/50)	Between 440 mm ~1000-1150 mm	Between 5060 cm ² ~11500-22195 cm ²	Between 0.54-1.20 MPa ~0.32-1.40 MPa
Roeder et al. [3]							
5.	14x Specimens on embedded steel profiles W10x45 L=750-1675 mm W10x22 L=1220 mm W10x77 L=1270 mm	Circ. column Ø500 and Encasement 450x450 $f_c = 35 \text{ MPa}$ Age: 28 days	Blast cleaned to remove mill scale, cleaned with degreaser Trisodium Phosphate	Concrete cover. Dir. 1: 90-122 mm Dir. 2: 96-152 mm Stirr: Ø3/200, Ø3/75 Spiral: Ø3/75	Between 600-1525 mm	Between 7861-19978 cm ²	Between Average: 0.88-1.32 MPa Local: 2.20-2.75 MPa
Xing et al. [4]							
6.	18x Specimens on embedded steel bars: Ø8 L=550 mm, Ø14 L=550 mm, Ø16 L=550 mm	Cube 200 mm $f_c = 40.8-48.5 \text{ MPa}$ Age: 28 days	No	Concrete cover. 92-96 mm	Between 80-160 mm	Between 20-80 cm ²	Between 2.22-5.51 MPa (one series with 0.25 MPa)
SmartCoCo [5]							
7.	2x Specimens on HEB120 embedded steel profiles L=1100 mm	C40/50 Block 340x1000x1000 $f_c = 71 \text{ MPa}$ Age: 28 days	Variant 1: Rusted profile Variant 2: Coated with paint	Concrete cover. Dir. 1: 440 mm Dir. 2: 110 mm Stirrups: Ø12/150	900 mm	6174 cm ²	Between 1.34 MPa (Paint) 2.91 MPa (Rust)
Tao et al. [6]							
8.	20x Concrete-filled tubes circular and rectangular section Rectangular D120-600 Circular Ø120-400	Tube infill $f_c = 42-81.8 \text{ MPa}$ Age: 31-1176 days	For carbon steel: untreated surface For stainless steel: 2B and 2K finishing (EN10088-4:2009 [19])	External tube cover. rectangular circular	Between 600-1800 mm	Between 2111-41760 cm ²	Between 0.42-1.85 MPa (some series 0.03-0.33 MPa)
Pecce et al. [7]							
9.	14x Partially embedded HEB180 L=630 mm	Partial embeddm. $f_c = 22-35 \text{ MPa}$ Age: no information	Untreated and Oiled	Space between the flanges of the steel profile	450 mm	2990 cm ²	Between 0.05-0.45 MPa (flange contact only 0.1-0.75 MPa)

Xu et al. [8]							
10.	7x Concrete-filled rectangular tubes D180 and L=600 mm	Tube infill Expansive mix. f_c no information Age: 33 days	No information	External tube cover	580 mm	3990 cm ²	Between 0.36-0.55 MPa
Nardin et al. [9]							
11.	1x Concrete-filled rectangular tube D200 and L=425 mm	Tube infill f_c =48 MPa Age: no information	No information	External tube cover	375 mm	2811 cm ²	0.22 MPa
Mollazadeh [10]							
12.	5x Concrete-filled rectangular tubes D150 and L=250-500 mm	Tube infill f_c =29-32 MPa Age: 28 days	Cleaned with alcohol	External tube cover	200 mm and 450 mm	1120 cm ² and 2520 cm ²	Between 0.20-0.26 MPa

* , Some results disturbed by a plastic deformation of the specimens applied beforehand – reused specimens after creep and shrinkage test of composite columns (see [1]).
 ~, Author refers to the evaluated chemical debonding stress values (values without friction mechanism) and no raw data available. Moreover, free slip prevented – specimen closed by end-plate. Given values approximated from the diagram (see [2]).